

Cronfa - Swansea University Open Access Repository

This is an author produced version of a paper published in:

Nature

Cronfa URL for this paper:

<http://cronfa.swan.ac.uk/Record/cronfa41093>

Paper:

Perry, C., Alvarez-Filip, L., Graham, N., Mumby, P., Wilson, S., Kench, P., Manzello, D., Morgan, K., Slangen, A., et al. (2018). Loss of coral reef growth capacity to track future increases in sea level. *Nature*, 558(7710), 396-400.

<http://dx.doi.org/10.1038/s41586-018-0194-z>

Should not be made publicly visible until 23 November 2018 (see <https://www.nature.com/authors/policies/preprints.html>)

This item is brought to you by Swansea University. Any person downloading material is agreeing to abide by the terms of the repository licence. Copies of full text items may be used or reproduced in any format or medium, without prior permission for personal research or study, educational or non-commercial purposes only. The copyright for any work remains with the original author unless otherwise specified. The full-text must not be sold in any format or medium without the formal permission of the copyright holder.

Permission for multiple reproductions should be obtained from the original author.

Authors are personally responsible for adhering to copyright and publisher restrictions when uploading content to the repository.

<http://www.swansea.ac.uk/library/researchsupport/ris-support/>

1 Loss of coral reef growth capacity to track future increases in sea-level

2
3 Chris T Perry^{1*}, Lorenzo Alvarez-Filip², Nicholas AJ Graham³, Peter J Mumby⁴, Shaun K. Wilson^{5,6}, Paul S Kench⁷, Derek P
4 Manzello⁸, Kyle M Morgan⁹, Aimee BA Slangen¹⁰, Damian P Thomson¹¹, Fraser Januchowski-Hartley¹², Scott G Smithers¹³,
5 Robert R Steneck¹⁴, Renee Carlton¹⁵, Evan E Edinger¹⁶, Ian C Enochs^{8,17}, Nuria Estrada-Saldívar², Michael DE Haywood¹⁸,
6 Graham Kolodziej^{8,17}, Gary N Murphy¹, Esmeralda Pérez-Cervantes², Adam Suchley², Lauren Valentino^{8,17}, Robert
7 Boenish¹⁹, Margaret Wilson²⁰, Chancey Macdonald^{21,22}

8 ¹ Geography, College of Life and Environmental Sciences, University of Exeter, Exeter, UK;

9 ² Biodiversity and Reef Conservation Laboratory, Unidad Académica de Sistemas Arrecifales, Instituto de Ciencias del Mar y
10 Limnología, Universidad Nacional Autónoma de México, Prol. Av. Niños Héroes, C.P. 77580, Puerto Morelos, Quintana
11 Roo, Mexico

12 ³ Lancaster Environment Centre, Lancaster University, Lancaster, LA1 4YQ, UK

13 ⁴ Marine Spatial Ecology Lab, School of Biological Sciences, University of Queensland, Brisbane, Queensland 4072,
14 Australia

15 ⁵ Department of Biodiversity, Conservation and Attractions, Kensington, Perth, Western Australia, Australia.

16 ⁶ Oceans Institute, University of Western Australia, Crawley, WA 6009, Australia.

17 ⁷ School of Environment, The University of Auckland, Private Bag 92019, Auckland, New Zealand

18 ⁸ Atlantic Oceanographic and Meteorological Laboratory, NOAA, 4301 Rickenbacker Cswy., Miami, FL 33149 USA

19 ⁹ Asian School of the Environment, Nanyang Technological University, 50 Nanyang Avenue, Block N2-01C-37, Singapore
20 639798

21 ¹⁰ NIOZ Royal Netherlands Institute for Sea Research, Department of Estuarine & Delta Systems, and Utrecht University,
22 Koringaweg 7, 4401 NT, Yerseke, The Netherlands

23 ¹¹ CSIRO, Indian Ocean Marine Research Centre, 64 Fairway, Level 4, University of Western Australia, Crawley, WA, 6009,
24 Australia.

25 ¹² 2UMR 248 MARBEC/UMR250 ENTROPIE, UM2-CNRS-IRD-IFREMER-UM1, Université Montpellier 2, Montpellier,
26 France;

27 ¹³ School of Earth & Environmental Sciences, James Cook University, Townsville, Qld 4811 Australia

28 ¹⁴ School of Marine Sciences, University of Maine, Darling Marine Centre, Walpole, Maine 04573 U.S.A

29 ¹⁵ Khaled bin Sultan Living Oceans Foundation, Landover, MD USA

30 ¹⁶ Department of Geography and Department of Biology, Memorial University, St. John's, NL, A1B 3X9 Canada

31 ¹⁷ Cooperative Institute for Marine and Atmospheric Studies, Rosenstiel School of Marine and Atmospheric Science,
32 University of Miami, 4600 Rickenbacker Cswy., Miami, FL 33149 USA

33 ¹⁸ CSIRO, Oceans and Atmosphere, Queensland, Bioscience Precinct, 306, Carmody Road, St Lucia, Qld 4067, Australia.

34 ¹⁹ University of Maine, School of Marine Sciences, Orono, ME 04469, USA

35 ²⁰ Bren School of Environmental Science & Management, University of California, Santa Barbara, Santa Barbara, CA 93106,
36 USA

37 ²¹ ARC Centre of Excellence for Coral Reef Studies, James Cook University, Queensland 4811, Australia

38 ²² Marine Biology and Aquaculture Science, College of Science and Engineering, James Cook University, Townsville, 4811,
39 Australia.

40 * Corresponding author: c.perry@exeter.ac.uk

41 **Sea-level rise (SLR) is predicted to elevate water depths above coral reefs and to increase coastal wave exposure**
42 **as ecological degradation limits vertical reef growth, but projections lack local reef growth-sea level interaction**
43 **data. Here we calculate the vertical growth potential of >200 Tropical Western Atlantic and Indian Ocean reefs, and**
44 **compare these against recent and projected rates of SLR under different Representative Concentration Pathway**
45 **(RCP) scenarios. Whilst many reefs retain accretion rates close to recent SLR trends, few will have capacity to track**
46 **SLR projections under RCP 4.5 scenarios without sustained ecological recovery, whilst under RCP 8.5 most reefs**
47 **are predicted to experience mean water depth increases >0.5 m by 2100. Coral cover strongly predicts reef capacity**
48 **to track SLR, but threshold cover levels necessary to prevent submergence are well above those observed on most**
49 **reefs. Urgent action to mitigate climate, sea-level and future ecological changes are thus needed to limit**
50 **magnitudes of future reef submergence.**

51

52 Sea-level rise (SLR) will directly impact coastal communities through shoreline inundation and erosion^{1,2}. Along coral reef
53 fronted coastlines the maintenance of reef surface elevation relative to sea-level will critically influence magnitudes of future
54 shoreline change and flooding risk^{3,4}. This is because reef structure and water depth modulate across-reef and nearshore
55 wave energy regimes⁵⁻⁷. Mean water depth increases will occur where vertical growth rates lag behind actual or relative
56 (e.g., from glacial isostatic adjustment or land subsidence) increases in sea-level^{4,8}. This is a widely discussed scenario as
57 reef-building species abundance declines globally, limiting reef growth potential⁹⁻¹⁴, whilst at the same time significant sea
58 level increases are projected (global mean 0.44 m under RCP2.6 by 2100, 0.74 m under RCP8.5 [Representative
59 Concentration Pathways^{15]}¹⁶. Even modest depth increases of ~0.5 m above reefs are projected to increase coastal flooding
60 risk, and change nearshore sediment dynamics^{3,5,17,18}. However, datasets to support predictions of magnitudes of above-
61 reef submergence and how these may vary geographically under different RCP scenarios are sparse²⁵. This is a major
62 knowledge gap with significant socio-economic and policy implications for urbanised tropical coastlines and reef islands
63 given projected costs of adaptation and mitigation planning⁴.

64

65 To estimate reef growth capacity under future SLR we calculated mean water depth increases above reefs using an
66 unprecedented dataset of reef carbonate budget data collected from >200 reefs around two major reef-building regions, the
67 Tropical Western Atlantic (TWA) and Indian Ocean (IO). These data, based on in-situ ecological metrics (see Methods),
68 were collected between 2009 and 2017 allowing us to explore intra-regional variations in contemporary carbonate budget
69 states and site specific temporal dynamics in budget states. Using these data we derived first-order estimates of maximum
70 vertical reef accretion potential (RAP_{max}) ($mm\ yr^{-1}$) (see Methods) to explore four key issues. First, we assess inter- and

intra-regional variations in site-specific RAP_{max} rates in the context of recent disturbance histories. Second, we use pre-and post-2016 bleaching datasets from impacted IO sites to quantify changes in RAP_{max} rates and consider the implications for reef growth given the increasingly important control bleaching has on reef health^{14,20,21}. Third, we derive best-estimate predictions of reef capacity to track projected rates of SLR, and project total minimum water depth increases at each site by 2100, by comparing site specific RAP_{max} rates against recent (1993-2010) altimetry-derived regional SLR rates and those projected under RCP4.5 and 8.5 scenarios²⁹. Fourth, we quantify the relationship between mean coral cover (as the most widely used reef “health” metric^{9,10}) and reef submergence under these same SLR scenarios over the next few decades to identify regional coral cover thresholds necessary to limit reef submergence.

Carbonate budgets and reef accretion potential

Our data show that contemporary carbonate budgets (G , where $G = \text{Kg CaCO}_3 \text{ m}^{-2} \text{ yr}^{-1}$) of most shallow water (<10 m depth) reefs across the TWA (mean \pm SD: $2.55 \pm 3.83 \text{ G}$) and IO (mean: $1.41 \pm 3.02 \text{ G}$) are currently low (Fig. 1A), and are substantially below optimal rates reported under high coral cover states for both regions (range ~5-10 G^{23}). Mean carbonate budgets do not differ significantly between the two ocean regions (GLMM; $p=0.485$), but there were significant differences among regions within ocean basins (GLMM; $p=0.046$). In the TWA highest carbonate budgets were calculated on Leeward Antilles reefs (mean \pm SD: $5.75 \pm 4.87 \text{ G}$; Fig. 1A), a rate closer to historical optimal rates²³. The lowest rates were along the Mesoamerican Reef (Mexico mean \pm SD: $0.14 \pm 3.81 \text{ G}$; Belize: $1.52 \pm 2.19 \text{ G}$), in Florida (mean \pm SD: $0.16 \pm 1.96 \text{ G}$) and Grand Cayman (mean \pm SD: $0.28 \pm 1.74 \text{ G}$; Fig. 1A; SI Table 1). These trends mirror those in coral cover reported in recent basin-wide analyses²⁴, and provide compelling evidence that both coral carbonate production (mean $4.22 \pm 4.06 \text{ G}$) and bioerosion rates (mean $1.74 \pm 1.46 \text{ G}$) are low across many TWA reefs. As with Net G there is marked intra-ocean variability (Extended Data Fig. 1) and we note that only sites in the south-east, such as Bonaire (Fig. 1B), are characterised by both high carbonate production and bioerosion rates (mean \pm SD: $8.12 \pm 4.60 \text{ G}$ and $2.79 \pm 1.08 \text{ G}$ respectively; see Extended Data Fig 1) that are close to historically estimated regional rates^{25,26}. In the IO, highest contemporary budgets were calculated on reefs in Mozambique (mean \pm SD: $4.78 \pm 5.01 \text{ G}$) and Ningaloo, Australia (mean \pm SD: $2.46 \pm 2.01 \text{ G}$). The lowest (and net negative) rates were calculated at Seychelles (mean \pm SD: $-1.51 \pm 1.90 \text{ G}$) and Maldives sites (mean \pm SD: $-2.98 \pm 1.30 \text{ G}$) (Fig. 1A; SI Table 1).

Low carbonate budget states are reflected in low calculated RAP_{max} rates at many sites across both oceans. In the TWA, the mean RAP_{max} rate across all sites is $1.87 \pm 2.16 \text{ mm yr}^{-1}$, but there is significant intra-ocean variability (GLMM; $p=0.032$).

Highest RAP_{max} rates were calculated from sites in the southern Lesser Antilles (mean \pm SD: $2.16 \pm 1.93 \text{ mm yr}^{-1}$) and

Leeward Antilles (mean \pm SD: 4.87 ± 2.71 mm yr⁻¹; Fig. 1B). Low RAP_{max} rates characterise all reefs examined in Florida and the Greater Antilles (Gd. Cayman 0.46 ± 0.66 mm yr⁻¹, Florida 0.19 ± 0.93 mm yr⁻¹; Fig. 1B) and along the Mesoamerican Reef (Belize mean \pm SD: 1.29 ± 0.89 mm yr⁻¹, Mexico 0.28 ± 1.52 mm yr⁻¹; Fig. 1B). These low RAP_{max} rates are likely to result from a prolonged period (at least multi-decadal in duration) of ecological decline driven by various regional-scale factors (fishing pressure, coral disease, bleaching, loss of herbivorous taxa, water quality declines^{13,27}) that have changed reef ecology.

In the IO, mean calculated regional RAP_{max} rates are only 2.01 ± 2.33 mm yr⁻¹. Sites in East Africa (Mozambique, mean \pm SD: 4.00 ± 2.78 mm yr⁻¹; Kenya, 1.72 ± 1.32 mm yr⁻¹) and Ningaloo, Western Australia (2.41 ± 2.01 mm yr⁻¹) have the highest mean RAP_{max} rates, whilst western and central IO sites are on average net negative (Seychelles, mean \pm SD: -0.43 ± 0.95 mm yr⁻¹; Maldives, -0.84 ± 0.47 mm yr⁻¹) (Fig. 1B). This reflects the fact that these areas were extensively impacted by the 2016 bleaching event (Extended Data Fig. 2), with widespread coral mortality to depths of at least 6-7 m²⁸. Chagos corals also suffered high mortality during 2016²⁹ and although post-event budget assessments have yet to be undertaken it is likely that the relatively high mean RAP_{max} rates we report (2.94 ± 2.06 mm yr⁻¹; Fig. 1) for Chagos far exceed contemporary rates. At sites with both pre- and post-2016 data, bleaching significantly reduced both Net G (GLMM; $p < 0.001$) and RAP_{max} (GLMM; $p < 0.001$). Declines were greatest in the Maldives and on “recovering reefs” (sensu Graham et al.³⁰) in the Seychelles (Extended Data Fig. 2). There were negligible differences on “regime shifted” Seychelles reefs as coral cover, Net G and accretion were already low. The major consequence of the 2016 event is that most reefs in the impacted areas are presently in net erosional or non-net accretionary states. Furthermore, given: 1) that not all Seychelles reefs recovered successfully from past (1998) bleaching³⁰; and 2) that models predict the rapid onset of annual bleaching for the central IO, under both RCP4.5 and 8.5 scenarios²¹ (i.e., well inside the timescales necessary for reef recovery^{31,32}) the capacity for IO reefs to regain high accretion states is increasingly questionable.

Reef accretion and projected sea level rise

To assess reef capacity to track local SLR we compared our calculated RAP_{max} rates against recent altimetry measured SLR rates for the period 1993–2010 (see Methods) and rates projected under RCP4.5 and 8.5²⁹ (see Methods; SI Table 2). In both regions only ~45% of reefs have calculated mean RAP_{max} rates close to (within ± 1 mm yr⁻¹) or above local recent (altimetry derived) SLR rates. Thus for many reefs there is already a divergence between reef growth potential and the local recent rate of SLR (Fig. 2). However, these values fall to only 6.2 % and 3.1% respectively in the TWA when we compare calculated RAP_{max} rates for each site to projected mean local RCP4.5 and 8.5 rates for the 21st century²². In the Indian

131 Ocean only 2.7% of reefs have mean RAP_{max} rates close to (within ± 1 mm yr^{-1}) RCP4.5 projections and 1.3% close to
132 mean RCP8.5 projections (Fig. 2). Whilst a more positive prognosis would be implied in the IO based on pre-bleaching
133 states (59% of the reefs had RAP_{max} rates close to (within ± 1 mm yr^{-1}) recent measured SLR rates; Fig. 2), our data
134 suggest that few reefs in either region will be able to match average 21st century projected SLR rates (see SI Table 2) if
135 current ecological conditions persist.

136

137 **Projections of reef submergence**

138 To assess magnitudes of future reef submergence we used our calculated RAP_{max} rates to predict total minimum water
139 depth increases above each reef by the end of this century (Fig. 3), and in the IO for selected sites based on pre- and post-
140 2016 bleaching data. These predictions are however likely at the more optimistic end of the spectrum in terms of reef keep-
141 up capacity, both for methodological reasons (see Methods) and because of the lag time between climate warming and
142 SLR. Thus calculated magnitudes of water depth increase should be considered as best case scenarios and the minimums
143 for which regions should prepare. Allowing for these caveats our current projections are that if strong climate mitigation
144 actions can be rapidly implemented (e.g., an RCP2.6 type scenario) that restricts SLR rates to close to those measured
145 across our study areas over the last few decades (i.e., < 3 mm yr^{-1} ; see SI Table 2) then the difference between reef
146 accretion and SLR rate will on average be low in both regions assuming ecological conditions do not deteriorate further
147 (mean < 10 cm increases by 2100; see SI Table 3).

148

149 In contrast, significant water depth increases are projected above these reefs by 2100 under both RCP4.5 and 8.5
150 scenarios. Under RCP4.5 projections water depths on the TWA reefs are predicted to increase 14–66 cm (5–95% CI range)
151 (mean ~ 40 cm, or 4.8 mm yr^{-1}), and between 16–104 cm (5–95% CI range) (mean ~ 60 cm, or 7.2 mm yr^{-1}) under RCP8.5
152 (Fig. 3). In the IO mean water depth is estimated to increase 14–72 cm (5–95% CI range) (mean 47 cm, or 5.6 mm yr^{-1})
153 under RCP4.5, and between 22–112 cm (5–95% CI range) (mean 71 cm, or 8.5 mm yr^{-1}) under RCP8.5 (Fig. 3; SI Table 3).
154 Larger average increases of ~ 63 cm under RCP4.5 (34–92 cm, 5–95% CI range) and 87 cm (41–132 cm, 5–95% CI range)
155 under RCP8.5 (Fig. 3; SI Table 3) are predicted for bleaching impacted central IO reefs in the absence of sustained
156 ecological recovery. The major implications are that whilst 32% of TWA and 45% of IO reefs are predicted to experience
157 increases of > 0.5 m by 2100 under mean local RCP4.5 scenarios, under RCP8.5 projections 80% of our TWA and 78% of
158 IO reefs are predicted to experience minimum mean water depth increases above this level. This is an important depth
159 threshold as recent models suggest that, on average, wave energy regimes will increase especially rapidly once water depth
160 increases exceed 0.5 m³³. Of major future concern is that due to the delayed response of processes contributing to SLR,

(deep ocean warming, ice sheet and glacier mass loss), these submergence trends are projected to increase towards the end of the century^{16,22,34}. Thus the higher end projections of water depth increases for each scenario may be more realistic (SI Table 3), rapidly exacerbating the threat to coastal communities and to Small Island Developing States^{1,4}.

Reef state and submergence trajectories

An especially pressing issue for reef and coastal managers is the question of which reefs are most likely to experience submergence over the coming decades, and how does this relate to reef state? Percent live coral cover is the most widely-reported metric of reef state and we thus used our data to examine whether a metric as simple as coral cover had predictive capacity for projecting changes in sea-level above reefs. Although our data sets span two biogeographic provinces, a range of depths (2 to 13 m), and a diversity of community structures, coral cover explained up to 62% of the projected increase in net water depth by the year 2050 (Fig. 4, Extended Data Table 1). Simulations uncover that high coral cover states would experience little water depth increase with some even extending closer to the surface. However, statistical fits to our data suggest that coral cover levels of ~40% in the TWA, and ~50% in the IO, are needed to avoid the prospect of net reef submergence in the next few decades (by 2050) under mean RCP4.5 SLR projections, but that this threshold rises to nearly 60% in the TWA and nearly 70% in the IO under the current emissions trajectory of RCP8.5. Given that coral cover levels across the sites in our dataset average only $20.6 \pm 13.9\%$ in the TWA, and $17.8 \pm 12.6\%$ in the IO region (SI Table 1), there is thus a high probability that mean water depths above reefs will increase by at least a few tens of centimetres in the coming decades.

Summary

The potential for a high proportion of reefs (>75% across our sites under RCP8.5) to experience water depth increases greater than 0.5 m by 2100 is of concern, because modelling studies suggest this will be sufficient to open higher wave energy windows that will increase sediment mobility, shoreline change and island overtopping^{1-3,17,18}. We also show that major climate-driven perturbations, specifically coral bleaching, can drive major declines in reef accretion potential. The most worrying end-point scenario is that if predictions of increasing bleaching frequency are realised^{21,35} and result in more frequent mortality, reefs may become locked into permanent low accretion rate states, leading to increasing rates of submergence under all SLR scenarios. Ocean acidification and thermal impacts on calcification represent additional threats and may negatively impact reef calcification and increase bioerosion^{36,37}. These collective threats will be exacerbated by the low coral cover states that define many reefs, and which our analysis suggests will be insufficient to prevent reef submergence. Our approach represents a first step in improving our predictive capabilities in these areas, but given the

societal relevance and economic costs of SLR along populated tropical coastlines⁴, and that coral reefs have the potential to play a key role in nature-based defence strategies, these issues should have high priority on the research agenda.

Acknowledgements

We thank the many local institutions that supported and facilitated field data collection. Data collection in the TWA was supported through a Leverhulme Trust International Research Network grant (F/00426/G) to C.T.P., and specifically in Mexico through a Royal Society - Newton Advanced Research Fellowship (NA-150360) to L.A-F. and C.T.P.; in Florida and Puerto Rico as part of the National Coral Reef Monitoring Program through NOAA's Coral Reef Conservation Program and Ocean Acidification Program to D.M.; and in the eastern Caribbean through a National Geographic Research Grant to R.S.S.. Data collection in the Indian Ocean was supported: in Kenya and Mozambique through a NERC-ESPA-DFID: Ecosystem Services for Poverty Alleviation Programme Grant (NE/K01045X/1) to C.T.P.; in the Maldives through NERC Grant (NE/K003143/1) and a Leverhulme Trust Research Fellowship (RF-2015-152) to C.T.P.; in the Chagos Archipelago through a DEFRA Darwin Initiative grant (19-027); in the Seychelles through an Australian Research Council grant (DE130101705) and Royal Society grant (RS-UF140691) to N.A.J.G.; and in Ningaloo through the BHP-CSIRO Ningaloo Outlook Marine Research Partnership. P.J.M. acknowledges the Australian Research Council and World Bank/GEF CCRES project for funding. Rebecca Fisher (Australian Institute of Marine Science, Western Australia) provided statistical advice.

Online content Additional Extended Data display items and Supplementary Files are available in the online version of the paper.

Author contributions

C.T.P. conceived of the study with support from L.A-F, N.A.J.G, P.S.K and K.M.M.. C.T.P., N.A.J.G., P.S.K., K.M.M., P.J.M. A.B.A.S. and S.K.W. developed and implemented the analyses. C.T.P. led the manuscript and all other authors contributed data and made substantive contributions to the text.

Author information

Reprints and permissions information is available at www.nature.com/reprints. The authors declare no competing financial interests. Correspondence and requests for materials should be addressed to C.T.P. (c.perry@exeter.ac.uk)

References

1. Storlazzi, C.D., Elias, E.P.L. & Paul Berkowitz, P. Many atolls may be uninhabitable within decades due to climate Change. *Sci Reports* **5**, 14546 (2015).
2. Kench, P.S., Ford, M.R. & Owen, S.D. Patterns of island change and persistence offer alternate adaptation pathways for atoll nations. *Nature Comms* **9**, 605 (2018).
3. Beetham, E., Kench, P.S. & Popinet, S. Future reef growth can mitigate physical impacts of sea-level rise on atoll islands. *Earths Future* **5**, 1002–1014 (2017).
4. Ferrario, F. *et al.* The effectiveness of coral reefs for coastal hazard risk reduction and adaptation. *Nature Comms* **5**, 3794 (2014).
5. Baldock, T.E., Golshani, A., Callaghan, D.P., Saunders, M.I. & Mumby, P.J. Impact of sea-level rise and coral mortality on the wave dynamics and wave forces on barrier reefs. *Mar Poll Bull* **83**, 155–164 (2014).
6. Baldock, T.E. *et al.* Impact of sea-level rise on cross-shore sediment transport on fetch-limited barrier reef island beaches under modal and cyclonic conditions. *Mar Pollut Bull* **97**, 188–198 (2015).
7. Quataert, E., Storlazzi, C., van Rooijen, A., Cheriton, O. & van Dongeren, A. The influence of coral reefs and climate change on wave-driven flooding of tropical coastlines. *Geophys. Res. Lett.* **42**, 6407–6415 (2015).
8. van Woesik, R., Golbuu, Y. & Roff, G. Keep up or drown: adjustment of western Pacific coral reefs to sea-level rise in the 21st century. *Royal Society Open Sci.* **2**, 150181 (2015).
9. Bruno, J.F. & Selig, E.R. Regional decline of coral cover in the Indo-Pacific: Timing, extent, and subregional comparisons. *Plos One* **2**, e711 (2007).
10. Gardner, T.A., Côté, I.M., Gill, J.A., Grant, A. & Watkinson, A.R. Long-term region-wide declines in Caribbean corals. *Science* **301**, 958–960 (2003).
11. Perry, C.T. *et al.* Caribbean-wide decline in carbonate production threatens coral reef growth. *Nature Comms* **4**, 1402 (2013).
12. Perry, C.T. *et al.* Remote coral reefs can sustain high growth potential and may match future sea-level trends. *Sci. Rep.* **5**, 18289 (2015).
13. Kennedy, E.V. *et al.* Avoiding coral reef functional collapse requires combined local and global action. *Current Biology* **23**, 912–918 (2013).
14. Hughes, T.P. *et al.* Global warming and recurrent mass bleaching of corals. *Nature* **17**, 373–377 (2017).
15. Moss, R.H. *et al.* The next generation of scenarios for climate change research and assessment. *Nature* **463**, 747–756 (2010).

16. Church, J.A. *et al.* Sea Level Change in *Climate Change 2013: The Physical Science Basis. Contribution of Working Group I to the Fifth Assessment Report of the Intergovernmental Panel on Climate Change* (ed. Stocker, T.F. *et al.*) Cambridge University Press, Cambridge, United Kingdom and New York, NY, USA.
17. Storlazzi, C.D., Elias, E., Field, M.E. & Presto, M.K. Numerical modelling of the impact of sea-level rise on fringing coral reef hydrodynamics and sediment transport. *Coral Reefs* **30**, 83–96 (2011).
18. Beetham, E., Kench, P., O'Callaghan, J. & Popinet, S. Wave transformation and shoreline water level on Funafuti Atoll, Tuvalu. *J Geophys Res, Oceans* **121**, 311–326 (2016).
19. Yates, K.K., Zawada, D.G., Smiley, N.A. & Tiling-Range, G. Divergence of seafloor elevation and sea level rise in coral reef ecosystems. *Biogeosciences* **14**, 1739–772 (2017).
20. Hoegh-Guldberg, O. Climate change, coral bleaching and the future of the world's coral reefs. *Mar Fresh Res* **50**, 839–66 (1999).
21. van Hooidonk, R. *et al.* Local-scale projections of coral reef futures and implications of the Paris Agreement. *Sci. Reports* **6**, 39666 (2016).
22. Slangen, A.B.A. *et al.* Projecting twenty-first century regional sea-level changes. *Climatic Change* **124**, 317–332 (2014).
23. Vecsei, A. A new estimate of global reefal carbonate production including the fore-reefs. *Glob. Planet. Change* **43**, 1–18 (2004).
24. Jackson, J.B.C., Donovan, M.K., Cramer, K.L. & Lam, V.V. (eds.) *Status and Trends of Caribbean Coral Reefs: 1970-2012*. Global Coral Reef Monitoring Network, IUCN, Gland, Switzerland (2014).
25. Perry, C.T. *et al.* Regional-scale dominance of non-framework building corals on Caribbean reefs affects carbonate production and future reef growth. *Glob. Change Biol.* **21**, 1153–1164 (2014).
26. Perry, C.T. *et al.* Changing dynamics of Caribbean reef carbonate budgets: emergence of reef bioeroders as critical controls on present and future reef growth potential. *Proc. Royal Soc. B.* **281**, 2014–2018 (2014).
27. Mumby, P.J. & Steneck, R.S. Coral reef management and conservation in light of rapidly-evolving ecological paradigms. *Trends in Ecol. Evol.* **23**, 555–563 (2008).
28. Perry, C.T. & Morgan, K.M. Post-bleaching coral community change on southern Maldivian reefs: is there potential for rapid recovery? *Coral Reefs* **36**, 1189–1194 (2017).
29. Sheppard, C. *et al.* Bleaching and mortality in the Chagos Archipelago. *Atoll Res Bull* **613**, 26 pp (2017).
30. Graham, N.A., Jennings, S., MacNeil, M.A., Mouillot, D. & Wilson, S.K. Predicting climate-driven regime shifts versus rebound potential in coral reefs. *Nature* **518**, 94–97 (2015).

31. Sheppard, C.R.C. *et al.* Reefs and islands of the Chagos archipelago, Indian Ocean: why it is the world's largest no-take marine protected area. *Aquatic Conservation. Mar. Fresh. Ecosystems* **22**, 232–261 (2012).
32. Pisapia, C. *et al.* Coral recovery in the central Maldives archipelago since the last major mass-bleaching, in 1998. *Sci Reports* **6**, 34720 (2016).
33. Siegle, E. & Costa, M.B. Nearshore wave power increase on reef-shaped coasts due to sea-level rise. *Earth's Future* **5**, 1054–1065 (2017).
34. Carson, M. *et al.* Coastal sea level changes, observed and projected during the 20th and 21st century. *Climatic Change* **134**, 269–281 (2016).
35. Wolff, N.H. *et al.* Global inequities between polluters and the polluted: climate change impacts on coral reefs. *Glob. Change Biol.* **21**, 3982–3994 (2015).
36. Enochs, I.C. *et al.* Enhanced macroboring and depressed calcification drive net dissolution at high CO₂ coral reefs. *Proc. Royal Soc. B* **283**, 20161742 (2016).
37. Schönberg, C.H.L., Fang, J.K.H., Carreiro-Silva, M., Tribollet, A., Wisshak, M. Bioerosion: the other ocean acidification problem. *ICES J. Mar. Sci.* **74**, 895–925 (2017).

Figure captions

Fig. 1. Tropical Western Atlantic and Indian Ocean reef carbonate budgets and accretion rates. (a) Plots showing site level carbonate budget data ($\text{kg CaCO}_3 \text{ m}^{-2} \text{ yr}^{-1}$) grouped by country/territory within ecoregions. Box plots depict the median (horizontal line), box height depicts first and third quartiles, whiskers represent the 95th percentile, and outlier points are outside the 95th percentile. Bold numbers = country/territory (*italics* = *n* transects/site); (b) Calculated maximum reef accretion potential (RAP_{max}) rates (mm yr^{-1}) for each reef within ecoregions. Numbers in parentheses in each area box denote the country/territory followed by the mean accretion rate (mm yr^{-1}).

Fig. 2. Difference between calculated reef accretion potential (mm yr^{-1}) relative to recent (1993-2010) and projected rates of sea-level rise. Plots showing difference between reef accretion rate and sea-level rise (SLR) rate for (a) Tropical Western Atlantic (*n* = 95), and (b) Indian Ocean (*n* = 107) sites. Recent SLR rates are based on altimetry data for the period 1993 – 2010 (see Methods). Mean RCP4.5 and 8.5 SLR rates (and 5% and 95% CI rates) are based on projections for the period 2018-2100²² (see SI Table 2). Dots show individual transect data within each site.

Fig. 3 Total predicted water depth increases above reefs by 2100. Plots for site level data showing predicted water depth increases against (a) mean RCP4.5, and (b) RCP8.5 sea-level rise projections for the period 2018-2100. Box plots depict median (horizontal line), box height depicts first and third quartiles, whiskers represent the 95th percentile, and outlier points are outside the 95th percentile. White bars denote pre-bleaching data. Bottom of grey boxed area shows the 0.5 m threshold above which significantly increased wave energy regimes are predicted. Site numbers as in Fig. 1.

Fig. 4. Relationships between mean coral cover (%) and changes in water depth (m) above reefs by 2050. Model simulations (100 per site and SLR scenario) showing for (a) Tropical Western Atlantic (*n* = 95 reefs), and (b) Indian Ocean sites (*n* = 104 reefs) predicted changes (y-axis) in mean water depth (m) above reefs as a function of coral cover (x-axis). Mean change in depth is shown as the centre point. Error bars are standard deviations. Simulations show trends under lower (5th percentile), mean, and upper (95th percentile) projections of SLR under RCP4.5 and RCP 8.5 sea-level rise scenarios.

Methods

Field data to calculate biological carbonate production and erosion rates, and from which net reef carbonate budgets (G , where $G = \text{kg CaCO}_3 \text{ m}^{-2} \text{ yr}^{-1}$) could be calculated were collected from reef sites spanning both the Tropical Western Atlantic (TWA) and Indian Ocean (IO) regions. All data were collected between 2009 and 2017 (see SI Table 1). At most TWA sites these data were collected using the ReefBudget methodology³⁸, and for IO sites using a previously reported adapted version of this methodology^{12,39} that factors for regional differences in coral assemblages and bioeroding communities. Data were collected through a number of discrete projects, but in all cases the aim was to capture data from the main shallow water reef-building zones within a range of sites within each country. Survey depths and habitat types thus reflected this variability, although were kept as consistent as possible within countries, and replicate transects within sites were always depth-consistent. In the TWA, data were mostly collected within the 8-10 m depth fore-reef zone but, where field/logistical conditions allowed, also at shallower (~5 m depth) sites, although the number of locations where data from both depths could be collected was limited. In the IO region survey depths and habitat zones are more variable reflecting the more diverse range of reef types and geomorphologies associated with the countries in our dataset. Our data thus provide an overview of the range in budgetary states, and the resultant accretion potential, of reefs within a country, accepting that not every reef or setting can be realistically assessed. No budget data were collected from high energy reef crest settings (<2 m depth) due to physical working constraints, but we note that reported long-term accretion rates for such settings (where these systems are usually dominated by coralline algae) are generally <1-2 mm yr⁻¹^{40,41}, rates that are not dissimilar to those calculated at many sites in this study. The number of replicate transects (see SI Table 1) varied between sites (range 3 to 8) depending on field logistics and weather constraints.

Following the ReefBudget methodology benthic data were collected using a 10 m transect as a guide line below which a separate 1 m flexible tape was used to measure the distance within each linear 1 m covered by each category of benthic cover. All overhangs, vertical surfaces and horizontal surfaces below the line were thus surveyed. Scleractinian corals were recorded to species level in the TWA, and to genera and morphological level (e.g., *Acropora* branching, *Porites* massive etc.) in the IO. Substrate rugosity was calculated as total reef surface divided by linear distance (a completely flat surface would therefore have a rugosity of 1). To calculate rates of coral carbonate production we integrated mean percent cover of each coral species with species-specific (or nearest equivalent species) measures of skeletal density (g cm^{-3}) and linear growth rate (cm yr^{-1}), as derived from published sources (see: <http://geography.exeter.ac.uk/reefbudget/>). These data were then combined with rugosity measures to yield a value for coral carbonate production (G) relative to actual transect surface area. For several sites in both regions carbonate production rates were calculated slightly differently because community composition data were based on standard linear intersect methodologies. These were TWA sites in the windward and leeward Antilles and, in the IO, at Ningaloo and Seychelles. In these cases individual coral colony cover data were scaled up to derive a 3-d measure of cover by using genera or growth form specific rugosity metrics. For several IO sites (Maldives and Seychelles) that were known to be severely impacted by the 2016 bleaching event we also report post-bleaching changes in carbonate production rates, with census data collected using the same methodology as that used pre-bleaching.

To calculate rates of bioerosion we also undertook census studies to determine abundance and size of parrotfish and bioeroding urchins (both to species level) per unit area of reef following the methods previously reported for TWA and IO sites^{12,38}. All parrotfish abundance data were collected along replicate 30 x 4 m belt transects, except in Chagos (50 x 5 m belts), Seychelles (7.5 m radial surveys) and Ningaloo (100 x 10 m belts). To calculate bioerosion rates by each individual

fish we used models based on total length and life phase to predict the bite rates (bites hr⁻¹) for each species, as reported in Perry et al.^{12,38}. To calculate bioerosion rates by urchins we undertook additional surveys at each site, using either 10 x 2 m or 10 x 1 m belt transects to determine the species and test sizes of urchins per unit area of reef. Census data were then combined with published species/test class size erosion rate data^{12,38} to yield a measure of erosion rate. Rates of endolithic bioerosion were estimated for most TWA sites based on a census of endolithic sponge tissue cover per unit area of reef substrate^{38,42}. Exceptions were sites in Bonaire and the Windward Antilles where surveys were not conducted and literature-derived rates from the TWA were applied. Endolithic bioerosion rates were estimated at all IO sites by applying rates from the literature to available benthic substrate¹².

To calculate maximum reef accretion potential (RAP_{max}) rates (mm yr⁻¹) at each site we followed a previously used method^{11,12} based on the conversion of measured site specific net carbonate production rates (G) as proposed by Smith & Kinsey⁴³. In this conversion net carbonate production is taken as the sum of calculated gross carbonate production by corals and coralline algae less erosion rate. We then also factored for variations in accumulating reef framework porosity as a function of coral community type and for sediment reincorporation⁴³. Stacking porosity values ranging from ~80% for branching coral assemblages to ~20 % for head coral dominated assemblages, with rates of ~50% for mixed assemblages were proposed in the original work⁴⁴. However, since coral communities are rarely entirely monospecific we used the following rates in our calculations: 30% for head and massive coral dominated assemblages, 70% for branched and tabular dominated assemblages, and 50% for mixed coral assemblages (based on data in Kinsey & Hopley⁴⁴) as determined for each site from benthic coral community data. Sediment reincorporation was factored for by allowing for a proportion of the bioeroded framework (that is converted to sediment) to be reincorporated back into the accumulating reef structure. This proportion was calculated as the sum of 50% of the parrotfish-derived sediment (as a highly mobile bioeroder which defecates randomly over the reef), as well as all sediment produced by urchins and by macrobioerosion. To keep our estimates conservative we worked on the assumption that only ~50% of this bioerosional sediment yield is actually incorporated back into the reef (see also ref 45), and excluded any sediment generation by other benthic sediment producers (e.g., *Halimeda*).

Due to the absence of empirical data on rates of physical reef framework removal per unit area of reef surface over time we did not factor for physical loss rates. For the same reason we also did not factor for chemical dissolution of the substrate. The accretion rates we report, which we consider as current best-estimates of accretion potential across the entire upper portion of a reef profile (on the basis that accretion can result from both in-situ coral accumulation and the supply of physically-derived rubble from shallow fore-reef areas to the crest/flat⁴⁶, are thus defined as a rate of maximum reef accretion potential, or RAP_{max}). We thus consider these rates to represent the upper limits of how fast reefs may be accreting at present, and acknowledge that if physical framework loss and chemical dissolution rates⁴⁷ could be appropriately factored for at the site level our projected rates would likely be lower. How much lower will depend on spatial variations in physical disturbance regimes and the susceptibility of coral taxa to physical disturbances, and both are likely to vary markedly at intra-regional scales. Testing the validity of our high end (RAP_{max}) rates is thus not simple.

Evidence from Holocene core records of reef growth, when ecological conditions (in terms of the abundance of high rate carbonate producing taxa, e.g., *Acropora* spp.) are considered to have been more optimal, suggest that many reefs exhibited an impressive capacity to either “keep-up” or to “catch-up” during periods of past rapid SLR. Indeed, calculated

vertical accretion rates from the early Holocene, when sea-levels were rising rapidly, may have been as high as 12-15 mm yr⁻¹ in both the TWA and IO regions⁴⁸. Whilst longer term average accretion rates were lower (e.g., ~3-4 mm yr⁻¹ in the TWA⁴⁹; and a little below this in the IO region⁴⁸) these still exceed those estimated for many modern reefs in our dataset, and fall well below even mean RCP 4.5 SLR scenarios (see SI Table 2). Furthermore, reef core studies that might allow some assessment of very recent accretion histories on a site-by-site basis i.e., with a focus on the last couple of hundred years of reef growth, are sparse/absent and would make for inherently problematic comparisons because of the magnitudes of coral community change that have occurred at most sites over the last few decades.

However, one useful (albeit sub-area specific) comparator is the recent work of Yates et al. (ref 19) which used historical bathymetric data from the 1930s to 1980s and Lidar-derived Digital Elevation Models from the late 1990s to 2000s in Florida to calculate net changes in seafloor elevation. This data integrates for the effects of any physical and chemical losses and suggests net negative accretion rates in the Upper Florida Keys of around -1.5 mm yr⁻¹ (over the past 68 years), of -4.5 mm yr⁻¹ in the Lower Florida Keys (over the past 66 years) and of -2.7 mm yr⁻¹ in the US Virgin Islands (over the past 33 years). Our data from different sites in this region (SE Florida, the upper Florida Keys and the Dry Tortugas) and which do not include data from lagoon sands and seagrass beds that were integrated within the Yates et al. study, have average contemporary accretion rates of -0.4, 1.7 and 0.8 mm yr⁻¹ respectively. Our rates are thus, as expected for the various reasons outlined above, a little higher but are not markedly higher, suggesting they provide a reasonable estimate of high end reef accretion potential.

To test for differences in Net G and calculated accretion rates between sites and countries across our dataset we fitted generalized linear mixed models (GLMMs) to assess if rates were statistically significantly different between oceans and regions (n = 885 transects), as well as for the effects of bleaching and the interaction with location (Maldives, Seychelles recovering and regime shifted) (n = 338 transects), whilst controlling for site depth and the random effect of site. All GLMMs were fitted using a Gaussian distribution via the lmer function from package lme4⁵⁰ in R⁵¹, with significance assessed using F-ratio statistics calculated via the Anova function in the CAR⁵² package. Model assumptions of normality and homogeneity of variance were assessed graphically and found to be adequately met. We found a very weak effect of depth on Net G (and thus RAP_{max} rates) across our dataset, with Net G typically being slightly higher on the deeper reefs (p=0.001, r = 0.160). Although our datasets do not allow a detailed consideration of this issue at the within-region level, the fact that average accretion rates do not noticeably decline with depth across the upper fore-reef depth internals is consistent with trends inferred from Holocene core records in the TWA region⁴⁹.

To assess the capacity of the reefs in our datasets to match recently observed and future projected changes in sea level, and to estimate magnitudes of water depth increases relative to projected reef accretion by 2100 at each site, we compared our calculated RAP_{max} data against local sea-level change data (SI Table 2). In these comparisons we assume steady state ecological conditions persisting. For recent observed rates of change we compared our RAP_{max} rates against altimetry data for the period 1993-2010 from combined TOPEX/Poseidon, Jason-1, Jason-2/OSTM and Jason-3 satellite altimetry fields (downloaded from http://www.cmar.csiro.au/sealevel/sl_data_cmar.html on 22 January 2018). The fields used are monthly averages on a 1x1° grid with the seasonal (annual and semi-annual) signal removed and include inverse barometer and GIA corrections. The observed rates were computed by fitting a linear trend to the monthly 1993-2010 time series at the nearest available ocean grid point to the reef location. For the period 2018-2100 we used sea-level projections under the RCP4.5

and RCP8.5 scenarios^{22,34}. These regional sea-level projections factor for changes in ocean density and dynamics, changes in atmospheric pressure, and glacier and ice sheet surface mass balance contributions based on output from 21 CMIP5 atmosphere-ocean coupled climate models (Climate Model Intercomparison Phase 5⁵³). In addition, the projections account for model-based contributions from anthropogenic groundwater extraction, for glacial isostatic adjustment and observation-based estimates of ice sheet dynamical processes. The regional sea-level patterns of mass redistribution account for changes in gravitational, deformational and rotational feedbacks. As for the recent observed rates of change, the spatial resolution of the SLR projections is 1x1° and the closest gridpoint (nearest neighbour) is extracted for comparison to the coral reef data (SI Table 2).

To obtain a greater insight into the importance of coral cover on near-future reef submersion, we undertook Monte Carlo simulations of carbonate budgets, potential accretion rates, and projected increases in depth under sea-level rise. One hundred simulations were carried out per site during which community structure was sampled randomly from the site-level statistical distribution of corals, CCAs, and sources of bioerosion (i.e., sampling from the observed mean and standard deviation of species-specific G or erosion rate at the site). Each simulation was extended to estimate the change in seawater depth at the year 2050 for six reference rates of sea-level rise (SLR) (as above): the 5th percentile, mean, and 95th percentile of the rate of SLR for each of two Greenhouse Gas (GHG) emission scenarios, RCP4.5 and RCP8.5. For each site, we obtained the mean and standard deviation for each of the six SLR references. Analyses of differences in accretion rate, rates of SLR, and increases in depth over reefs were carried out using non-parametric mixed effects models based on Euclidean distance⁵⁴. This technique is analogous to parametric linear mixed effects models but makes no assumptions about the statistical distribution of errors. Fixed effects included biogeographic region (TWA vs IO), GHG emissions scenario (RCP4.5 vs RCP8.5), and coral cover. Country was added as a random effect nested within biogeographic region. The only exception to this approach was the use of linear mixed effects models in order to estimate threshold levels of coral cover where the net submergence of reefs was zero. Models were fitted using the same structure as in PERMANOVA but the predict function was used to estimate model fits for $y=0$ ⁵⁵. Analysis showed that a shift towards lower GHG emissions (RCP4.5) reduced the degree of reef submergence (Fig. 4, PERMANOVA; $p<0.001$) and emissions scenario gained in importance when switching from lower to mean to upper (95 percentile) bounds of projected SLR, explaining 2%, 44%, and 54% of the variance in reef submergence respectively (Extended Data Table 1). Under the upper bounds of SLR, biogeographic region also became significant (PERMANOVA; $p=0.005$) with submergence being somewhat greater in the IO (Fig. 4B). Under this pessimistic scenario, threshold levels of coral cover required to avoid net reef submergence were approximately 13% higher in the IO than the TWA (73% vs 60%) even under RCP4.5. This relative vulnerability of reefs in the IO was associated with higher rates of SLR (0.94 mm yr⁻¹ greater, PERMANOVA; $p=0.02$, Extended Data Tables 2, 3) rather than any biogeographic difference in accretion potential (PERMANOVA; $p=0.65$, Extended Data Table 4). While IO reefs are generally more resilient than those of the TWA⁵⁶, current ecological trajectories suggest that few coral reef locations will likely maintain sufficiently high coral cover levels to keep pace with future SLR, resulting in greater incident wave energy exposure, and changing spectrum of wave processes, along reef-fronted shorelines^{3,6}.

Data availability. Net carbonate budget and reef accretion rate data, and measured and projected sea-level data supporting the findings of this study are available within the paper and its supplementary information files. Site level coral cover and carbonate production and bioerosion datasets are available from the authors on request.

Additional references

38. Perry C.T. *et al.* Estimating rates of biologically driven coral reef framework production and erosion: a new census-based carbonate budget methodology and applications to the reefs of Bonaire. *Coral Reefs* **31**, 853–868 (2012).
39. Januchowski-Hartley, F.A., Graham, N.A.J., Wilson, S.K., Jennings, S. & Perry, C.T. Predicting divergent reef carbonate budget trajectories following a major climatic disturbance event. *Proc. Royal Soc. B* **284**, 20162533 (2017).
40. Steneck, R.S., Macintyre, I.G. & Reid, R.P. A unique algal ridge system in Exuma Cays, Bahamas. *Coral Reefs* **16**, 29–37 (1997).
41. Gherardi, D.F.M. & Bosence, D.W.J. Late Holocene reef growth and relative sea-level changes in Atol das Rocas, equatorial south Atlantic. *Coral Reefs* **24**, 264–272 (2005).
42. Murphy, G.N., Perry, C.T., Chin, P. & McCoy, C. New approaches to quantifying bioerosion by endolithic sponge populations: applications to the coral reefs of Grand Cayman. *Coral Reefs* **35**, 1109–1121 (2016).
43. Smith, S.V. & Kinsey, D.W. Calcium carbonate production, coral reef growth, and sea level change. *Science* **194**, 937–939 (1976).
44. Kinsey, D.W. & Hopley, D. The significance of coral reefs as global carbon sink-response to greenhouse. *Palaeogeog. Palaeoclim. Palaeoecol.* **89**, 363–377 (1991).
45. Hubbard, D.K., Miller, A.I. & Scaturro, D. Production and cycling of calcium carbonate in a shelf-edge reef system (St. Croix, U.S. Virgin Islands): applications to the nature of reef systems in the fossil record. *J. Sed. Petrol.* **60**, 335–360 (1990).
46. Blanchon, P. *et al.* Retrograde accretion of a Caribbean fringing reef controlled by hurricanes and sea-level rise. *Frontiers in Earth Science* **5**, 78 (2017).
47. Eyre, B.D., Andersson, A.J. & Cryonak, T. Benthic coral reef calcium carbonate dissolution in an acidifying ocean. *Nature Clim. Change* **4**, 969–976 (2014).
48. Dullo, W.C. Coral growth and reef growth: a brief review. *Coral Reefs* **51**, 33–48 (2005).
49. Hubbard, D.K. Depth- and species-related patterns of Holocene reef accretion in the Caribbean and western Atlantic: a critical assessment of existing models. *Spec. Publ. Int. Assoc. Sedimentol.* **40**, 1–18 (2008).
50. Bates, D., Maechler, M., Bolker, B. & Walker, S. Fitting Linear Mixed-Effects Models Using lme4. *J. Statistical Software* **67**, 1–48 (2015).
51. R Core Team. *R: A language and environment for statistical computing*. R Foundation for Statistical Computing, Vienna, Austria. URL <https://www.R-project.org/> (2017).
52. Fox J. & Weisberg, S. *An {R} Companion to Applied Regression*, Second Edition. Thousand Oaks CA: Sage. URL: <http://socserv.socsci.mcmaster.ca/jfox/Books/Companion> (2011)
53. Taylor, K., Stouffer, R.J. & Meehl, G.A. An overview of CMIP5 and the experiment design. *Bull Am Meteorol Soc* **93**, 485–498 (2012).
54. Anderson, M.J. A new method for non-parametric multivariate analysis of variance. *Austral Ecology* **26**, 32–46 (2001).
55. Pinheiro, J.C. & Bates, D.M. *Mixed-effects models in S and S-plus*. Springer-Verlag 528 pp (2000).
56. Roff G. & Mumby, P.J. Global disparity in the resilience of coral reefs. *Trends in Ecology & Evolution* **27**, 404–413 (2012).

EXTENDED DATA – Figure and table captions

Extended Data Figure 1. Tropical Western Atlantic and Indian Ocean coral carbonate production and bioerosion rates. Plots showing mean site level coral carbonate production rate (a), and bioerosion rate (b) data ($\text{kg CaCO}_3 \text{ m}^{-2} \text{ yr}^{-1}$) grouped by country/territory within ecoregions for Tropical Western Atlantic and Indian Ocean sites. Box plots depict the median (horizontal line), box height depicts first and third quartiles, whiskers represent the 95th percentile, and outlier points are outside the 95th percentile. Country/territory codes as follows: 1. Florida ($n = 36$), 2. Puerto Rico ($n = 6$), 3. Grand Cayman ($n = 26$), 4. Belize ($n = 36$), 5. Mexico ($n = 64$), 6. St. Croix ($n = 36$), 7. St. Maarten ($n = 11$), 8. Anguilla ($n = 10$), 9. Barbuda ($n = 20$), 10. Antigua ($n = 28$), 11. St. Lucia & St. Vincent ($n = 37$), 12. Bequia ($n = 12$), 13. Mustique ($n = 16$), 14. Canouan & Tobago Cays ($n = 20$), 15. Union/PSV and Carriacou ($n = 20$), 16. Bonaire ($n = 62$), 17. Mozambique ($n = 55$), 18. Kenya ($n = 29$), 19. Seychelles ($n = 144$), 20. Maldives ($n = 25$), 21. Chagos ($n = 111$), 22. Ningaloo ($n = 34$) ($n =$ number of transects per country/territory).

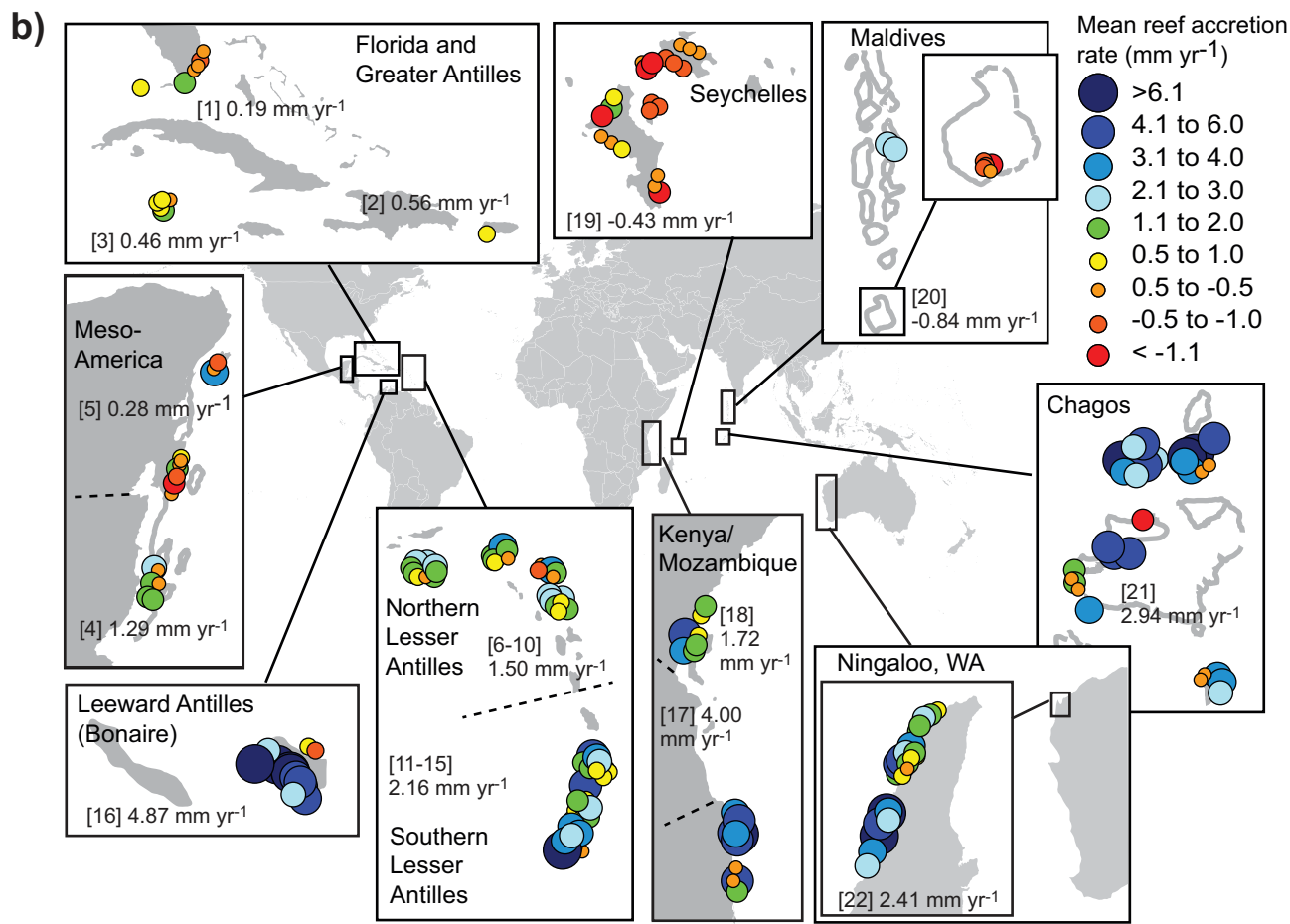
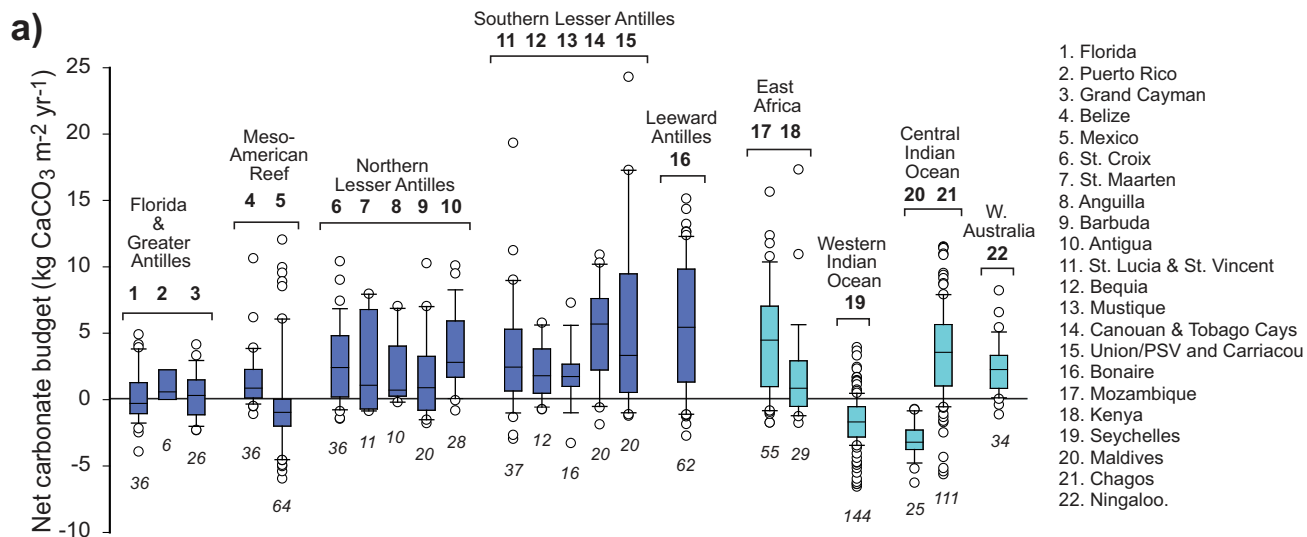
Extended Data Figure 2. Reef accretion pre- and post- the central Indian Ocean 2016 bleaching event. Calculated RAP_{max} rates (mm yr^{-1}) pre- (a, c) and post- (b, d) 2016 bleaching in the Seychelles and the Maldives. e) Plot shows changes in RAP_{max} rates and at “recovered” ($n = 96$) and “regime-shifted” reefs³⁸ ($n = 72$ pre-bleaching, $n = 48$ post-bleaching) in the Seychelles, and Maldives ($n = 35$ pre-bleaching, $n = 25$ post bleaching). Box plots depict the median (horizontal line), box height depicts first and third quartiles, whiskers represent the 95th percentile, and outlier points are outside the 95th percentile.

Extended Data Table 1. Effects of biogeography, coral cover, GHG emissions scenario, and range of SLR projection on the future submergence of coral reefs by 2050. Results of PERMANOVA analyses with coral cover, biogeographic region (TWA vs. TIO) and GHG emissions scenario (RCP4.5 vs RCP8.5) as fixed effects and country nested within (biogeographic) region as random effect.

Extended Data Table 2: Effect of Biogeographic Region on rates of SLR. PERMANOVA analysis testing the effect of biogeographic region on the upper 95% of predicted rates of SLR

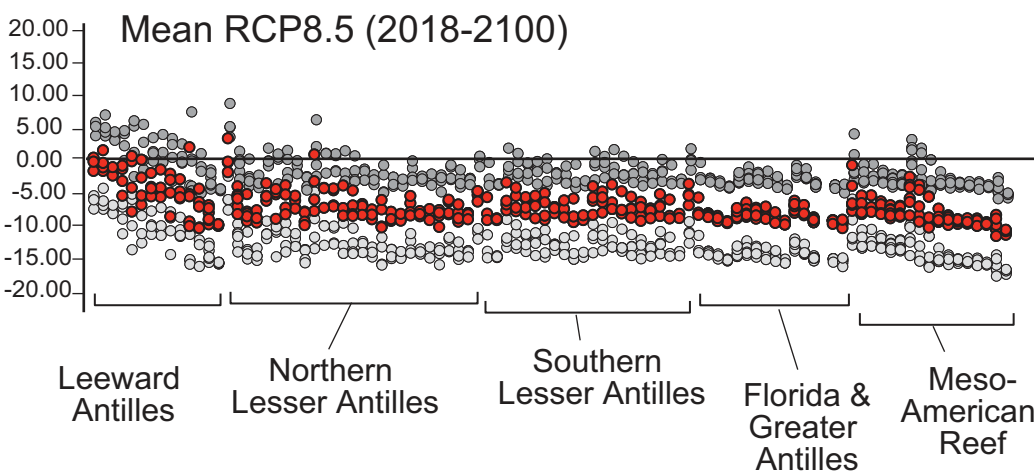
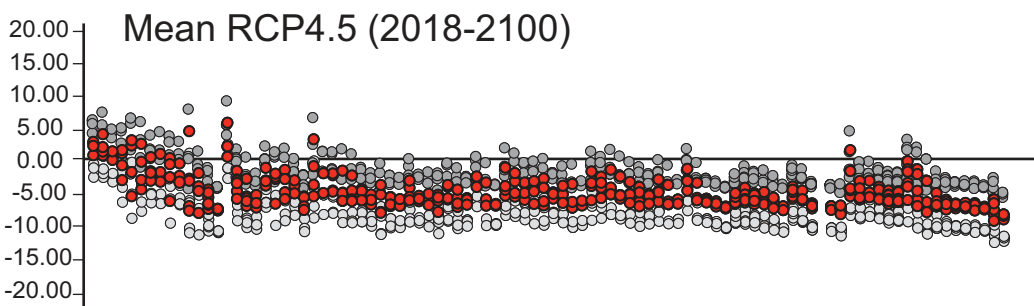
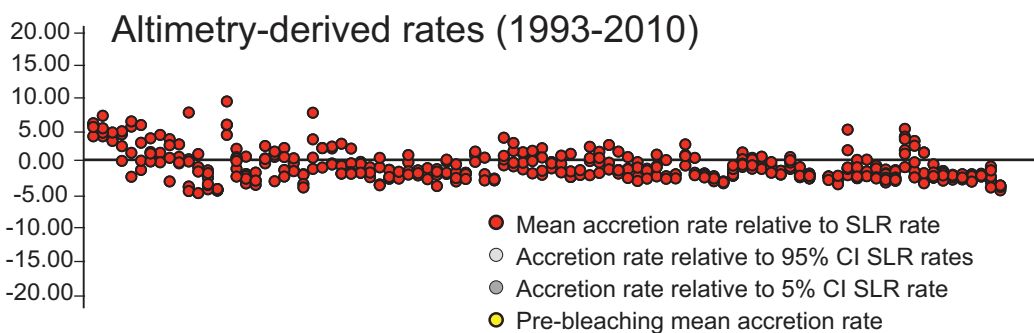
Extended Data Table 3: Differences between SLR rates between biogeographic regions (mm yr^{-1}). The difference in SLR rates between biogeographic regions (mm yr^{-1}) under two GHG emission scenarios and for all three components of SLR projections. Projections are higher in the Indian Ocean except in RCP4.5 lower percentile (0.03) which was non-significant.

Extended Data Table 4: Variability in potential accretion rate. Results of PERMANOVA analysis showing local (coral cover) versus regional (Tropical Western Atlantic vs. Indian Ocean) effects on the variability in potential accretion rate.



Difference (+ or -) between reef accretion potential rate (mm yr⁻¹) and local sea-level rise rate

a) Tropical Western Atlantic



b) Indian Ocean

